Formation of high density amorphous ice by decompression of ice VII and ice VIII at 135 K

Carl McBride, Carlos Vega, Eduardo Sanz, and Jose L. F. Abascal
Departamento de Química Física, Facultad de Ciencias Químicas, Universidad Complutense de Madrid, Ciudad Universitaria, 28040 Madrid, Spain

(Received 6 July 2004; accepted 16 September 2004)

Monte Carlo computer simulations of ice VII and ice VIII phases have been undertaken using the four-point transferable intermolecular potential model of water. By following thermodynamic paths similar to those used experimentally, ice is decompressed resulting in an amorphous phase. These phases are compared to the high density amorphous phase formed upon compression of ice I_h and are found to have very similar structures. By cooling liquid water along the water/I_h melting line a high density amorphous phase was also generated. © *2004 American Institute of Physics.*
[DOI: 10.1063/1.1814352]

I. INTRODUCTION

Twenty years ago Mishima, Calvert, and Whalley[1] observed that the melting curve of ice I_h extrapolates to ≈ 10 kbar at the liquid nitrogen temperature $T=77$ K. With this in mind an experiment was undertaken which squeezed ice I_h at 77 K. At 10 ± 1 kbars they saw the onset of a transition that was completed at around 15 kbar. The new phase was then recovered at room pressure. By using x-ray powder diffraction the specimen was found to have a halo pattern typical of an amorphous material. Having a density of 1.17 g cm^{-3} (at $T=77$ K and $p=1$ bar) led to its classification as a high-density amorphous ice (HDA). A few years later, the transition from ice I_h to the HDA phase was also obtained in computer simulations of water models.[2] Tse and co-workers suggested that the principal driving force for the crystalline to amorphous transition was mechanical instability of the ice I_h structure,[3] leading to "mechanical melting." Challenged by this suggestion, Mishima performed careful experimental measurements of the melting line of I_h from the triple point of water down to 77 K.[4] Mishima found a smooth crossover from pressure induced thermodynamic equilibrium melting for temperatures higher than 150 K (two phase melting) to a slow amorphisation of ice I_h (one phase melting) at temperatures below 150 K.

One of the salient points of these studies was that useful insights as to the location of solid/amorphous phase transitions can be obtained by extrapolation of melting curves. Of course it almost goes without saying that the extrapolation of melting curves to very low temperatures from the experimental melting curves at high temperatures is subject to uncertainty (as with any extrapolation).

In a similar vein to the extrapolation performed by Mishima, Klug *et al.*[5] extrapolated the melting lines for a number of ice structures to very low temperatures. Most of the melting lines of ice phases (III, IV, V, VI) intercept the zero pressure line at relatively high temperatures (as a corollary to this the extrapolated melting curve yields negative pressures at 77 K). The possibility of obtaining amorphous phases at low temperatures by decreasing the pressure in these high density ices appears unlikely. From an experimental point of view this presents certain advantages as it allows one to perform diffraction studies of the high pressure polymorphs at atmospheric pressure simply by quenching them in liquid nitrogen. The only extrapolated melting line with non-negative pressure at 77 K is that of ice VIII (the same is true for the melting curve of ice VII, however ice VII transforms into ice VIII when cooled). With this in mind Klug *et al.* were able to produce low density amorphous ice first by decompressing ice VIII at low temperatures and then heating to 125 K at ambient pressure. For an excellent review of the supercooled and glassy phases of water see Ref. 6.

In this work we shall use Monte Carlo simulations to check whether ice VII and ice VIII form amorphous phases (HDA) at low temperatures by isothermally decreasing the pressure. We shall show that this is indeed the case for both of these ices. It will be shown that the radial distribution functions of these HDA phases obtained upon expansion are virtually identical to those of the HDA phase obtained from compression of ice I_h.

II. SIMULATION DETAILS

Isobaric isothermal (N-p-T) Monte Carlo simulations were performed for several ices. The shape of the simulation box was allowed to vary using Parrinello-Rahman like volume changes.[7,8] The water model used was the well known four-point transferable intermolecular potential (TIP4P) potential.[9] The pair potential was truncated at 8.5 Å and standard long range corrections[10] to the Lennard-Jones energy were added. Electrostatic interactions were dealt with using the Ewald sum method.[10] Typically, equilibration and production stages consisted of 4×10^4 cycles each. One cycle consists of one trial move per particle and one trial volume change. The expansion runs were initiated at high pressures. Each subsequent simulation was started from the final configuration of the previous higher pressure run.

In ice VIII the protons are ordered.[11] This greatly facilitates the construction of the initial solid phase. The configu-

TABLE I. N-p-T simulation results for ice VII along the 135 K isotherm. Values for water cooled isobarically from 270 K (path 1) and by following the melting curve of ice I_h with a subsequent expansion at $T=135$ K (path 2) are shown for comparison.

Pressure	ρ/(g cm^{-3})	U/(Kcal/mol)	I_{hkl}	Phase
50 kbars	1.66	−10.29	0.487	Ice VII
40 kbars	1.61	−10.63	0.437	Ice VII
30 kbars	1.56	−10.92	0.379	Ice VII
20 kbars	1.49	−11.18	0.306	Ice VII
10 kbars	1.36	−11.63	0.028	HDA
1 bar	1.09	−11.90	0.004	HDA
1 bar	1.00	−12.09	0.020	Water (path 1)
1 bar	1.12	−11.96	0.037	Water (path 2)

ration from which the Monte Carlo simulations were initiated (at the highest considered pressure) was taken from the crystal structure obtained via neutron diffraction.[12]

In both ice I_h and ice VII the protons are disordered. While the oxygens are situated on the lattice points, the hydrogen atoms are located in disordered configurations such that the net dipole moment is zero as well as at the same time satisfying the ice rules.[13] Formation of such a structure was achieved by using the algorithm of Buch, Sandler, and Sadlej.[14] The number of molecules used in the simulations was $N=600$ molecules for ice VIII and $N=432$ for ice VII and ice I_h.

The loss of crystalinity was monitored by following the progression of the intensity of the Bragg reflection from the hkl planes of the crystal structure,

$$I_{hkl}=|F_{hkl}|^2=F_{hkl}F_{hkl}^*, \tag{1}$$

which is given by the square of the structure factor defined as

$$F_{hkl}=\frac{1}{N}\sum_{i=1}^{i=N} f_i \exp[2\pi i(hx_i+ky_i+lz_i)], \tag{2}$$

where x, y, and z are coordinates relative to the a, b, and c unit cell vectors. It should be mentioned that only oxygens were used when computing the structure factor in Eq. (2). The atomic scattering factor f_i of oxygen was arbitrarily set to 1. The most intense line was used to detect the loss of crystalinity, either because of a solid to liquid transition or due to the formation of an amorphous phase.

TABLE II. N-p-T simulation results for ice VIII along the 135 K isotherm. Values for water cooled isobarically from 270 K (path 1), by following the melting curve of ice I_h with a subsequent expansion at $T=135$ K (path 2) and by following the reference route are shown for comparison.

Pressure	ρ/(g cm^{-3})	U/(Kcal/mol)	I_{hkl}	Phase
40 kbars	1.70	−10.60	0.951	Ice VIII
30 kbars	1.66	−10.75	0.947	Ice VIII
20 kbars	1.61	−10.85	0.933	Ice VIII
15 kbars	1.59	−10.88	0.932	Ice VIII
10 kbars	1.56	−10.89	0.926	Ice VIII
5 kbars	1.52	−10.87	0.914	Ice VIII
2 kbars	1.18	−11.75	0.012	HDA
1 bar	1.09	−11.83	0.001	HDA
1 bar	1.00	−12.09	0.020	Water (path 1)
1 bar	1.12	−11.96	0.037	Water (path 2)
From I_h				
1 (I_h)	1.09	−11.90	0.003	HDA

TABLE III. N-p-T simulation results for ice VIII along the 225 K isotherm.

Pressure (kbar)	ρ/(g cm^{-3})	U/(Kcal/mol)	I_{hkl}	Phase
25	1.60	−10.29	0.893	Ice VIII
20	1.57	−10.30	0.881	Ice VIII
15	1.37	−10.92	0.021	Water
10	1.30	−10.95	0.009	Water

III. RESULTS

A summary of the N-p-T simulations for ice VII and ice VIII are presented in Tables I–III. For ice VII simulations were performed at $T=135$ K. For ice VIII simulations were performed at $T=135$ K and $T=225$ K. Note that at 50 kbars and 135 K ice VIII (and not ice VII) is the thermodynamically stable solid. However, due to the low temperature, ice VII is kinetically trapped in a metastable phase, being unable to reorder itself into ice VIII.

In Fig. 1 the equation of state is shown for ice VIII along the $T=135$ K isotherm. In Fig. 2 I_{hkl} is shown as a function of pressure. In the simulations of the ice VIII system, at a pressure of 2 kbars, the density of the system suddenly drops and the intensity of the reflection line decays to zero. From simple density considerations alone, it appears that the ice VIII phase has ''melted'' into a HDA ice. At first one would expect ice VIII to transform into ice I_h at low temperatures when the pressure decreases, given that ice I_h is the equilibrium thermodynamic state under these conditions. Ice I_h was never found when decompressing ice VIII or ice VII at low temperatures; the free energy barrier for such a transformation is very high, and is most unlikely to be overcome during simulations of the length described in this work.

In a manner analogous to the experimental route, a HDA phase was generated using computer simulation by following the route first proposed by Tse[3] and Okabe, Tanaka, and Nakanishi.[15] The system was compressed from the ice I_h phase at 1 bar along the 77 K isotherm. The compression took place at $p=1$, 2, 5, 8, 10, 12, 15, and 17 kbars. Between $p=10$ and 17 kbars the ice I_h phase melted into the HDA phase. Upon forming the HDA phase the pressure was isothermally reduced to 1 bar and the temperature then isobari-

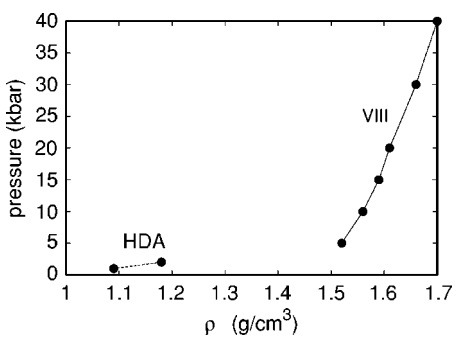

FIG. 1. Equation of state for ice VIII at 135 K. Dashed line is the HDA branch, solid line is the ice VIII branch.

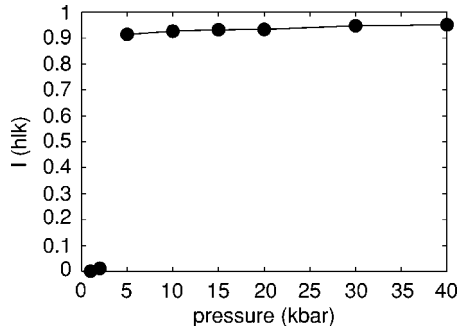

FIG. 2. Reflection intensity with respect to pressure for ice VIII at 135 K. The loss of crystallinity is clearly seen at low pressures.

caly raised to $T=135$ K. The HDA phase generated by following this recipe was used as the ''reference'' system against which the amorphous phases obtained upon expansion of ices VII and VIII were compared.

In previous simulation studies HDA was obtained by compressing ice I_h using the molecular dynamics technique.[3,15–17] In Fig. 3 a comparison is made between the Monte Carlo results of this work and the equation of state for the ice I_h and HDA branches from the molecular dynamics studies of Martoňák, Donaido, and Parrinello.[16] Good agreement between both sets of results is found.

It should be noted that time is not a variable in Metropolis Monte Carlo simulations. For this reason one is unable to derive time dependent properties. Thus, strictly speaking, one cannot define either heating or compression rates. However, one may relate one Monte Carlo cycle (one trial move for each particle/molecule) to one molecular dynamics time step since they both result in similar root mean square displacements. A typical molecular dynamics time step for water is 1 fs. With this in mind a typical Monte Carlo simulation of 100 000 cycles corresponds to roughly 100 ps. Thus a pressure change of 10 kbars over a period of 10 simulations leads to a compression rate of $\approx 1\times 10^{13}$ bars/s. A similar reasoning leads to 10^{11} K/s for heating rates. This is obviously much higher than typical experimental compression/heating rates, and should be borne in mind when comparing simulation results with experimental results.

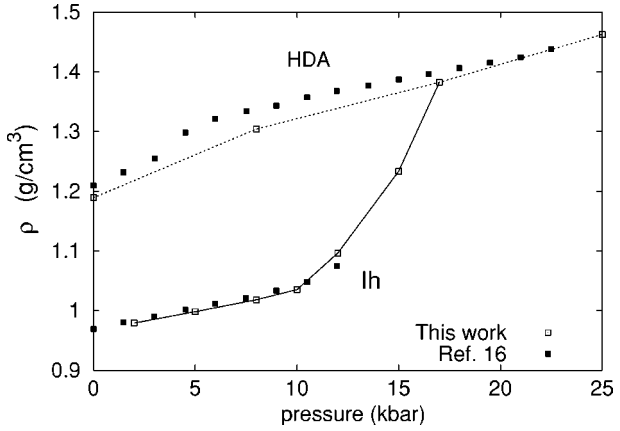

FIG. 3. Comparison for $T=77$ K between Monte Carlo results of this work (□) with data from molecular dynamics simulations (■) of Martoňák, Donadio, and Parrinello (Ref. 16). Solid line ice I_h equation of state. Dashed line HDA equation of state.

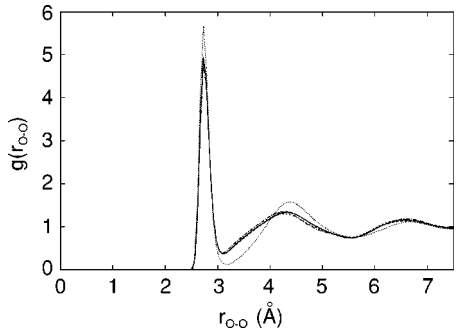

FIG. 4. Oxygen-oxygen site-site distribution function for HDA (I_h) (solid line), HDA(VII) (dashed line), HDA(VIII) (short dashed line), liquid water cooled from 270 to 135 K at 1 bar (path 1) (dotted line), and liquid water cooled via path 2 (dot-dashed line).

In Fig. 4 the oxygen-oxygen site-site correlation function of the HDA obtained from ice I_h [labeled as HDA(I_h)] is compared to the HDA(VII) and HDA(VIII). The agreement between the curves is excellent, especially with respect to the highly sensitive first peak. The same is true for the oxygen-hydrogen and hydrogen-hydrogen correlation functions (see Figs. 5 and 6). The density obtained for $T=135$ K and $p=1$ bar is $\rho=1.09$ g/cm^3 for the three HDA; HDA(I_h), HDA(VII), and HDA(VIII).

An interesting question is whether this HDA state can be obtained by cooling liquid water. Two distinct paths were followed from liquid water to the thermodynamic state $T=135$ K, $p=1$ bar. The first is an isobaric cooling at $p=1$ bar from liquid water at $T=270$ K down to $T=135$ K. This thermodynamic route will be denoted as path 1. The correlation functions resulting from path 1 are presented in Figs. 4, 5, and 6 (the dotted lines). It can be seen that they are markedly distinct from that of the HDA phase. The density of this supercooled water is $\rho=1.00$ g/cm^3.

A second route (path 2) was taken to reach this same state point. In path 2 the liquid water was cooled by following a series of pressure/temperature state points along the TIP4P ice I_h melting line. At $T=135$ K ($p=5780$ bars) the system was then isothermally expanded to a pressure of 1 bar (see Fig. 7). The site-site correlation function now coincides with the HDA functions in Figs. 4, 5, and 6, with a density of

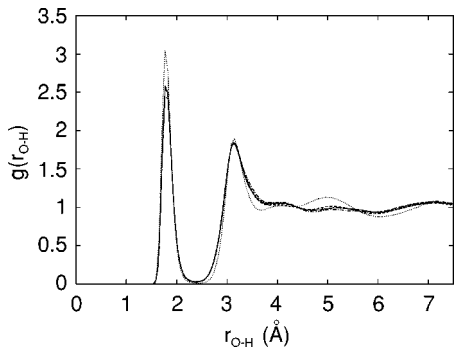

FIG. 5. Oxygen-hydrogen site-site distribution function. Symbols as in Fig. 4.

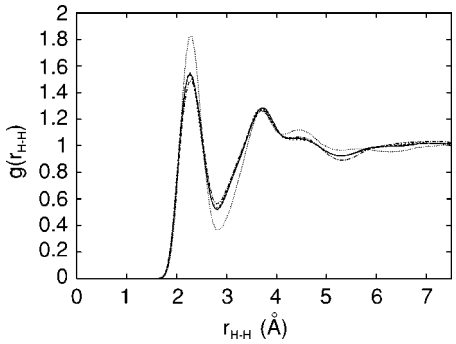

FIG. 6. Hydrogen-hydrogen site-site distribution function. Symbols as in Fig. 4.

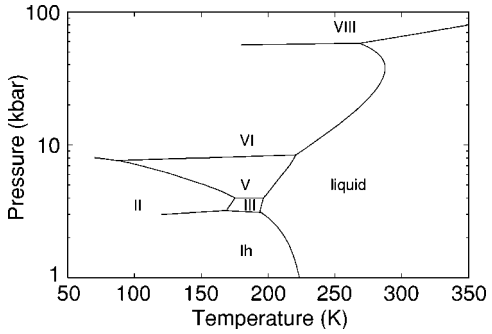

FIG. 8. Plot of a section of the TIP4P phase diagram (Refs. 20 and 21).

$\rho = 1.12$ g/cm^3. Apparently, upon isobaric cooling of liquid water at $p = 1$ bar a free energy barrier is encountered that cannot be overcome by the system, whereas cooling at an increased pressure reduces this barrier and allows supercooled water to reach a glassy phase similar to that of HDA. This is consistent with recent observations of Guillot and Guissani[17] and Giovambattista, Stanley, and Sciortino[18] for water, and of Morishita[19] for silicon.

The fact that the HDA structure can be obtained via four different routes (from ice I_h, from ice VIII, from ice VII and from liquid water along path 2) yielding the similar results suggests that the system has reached a local free energy minima.

The thermodynamic melting lines for both ice VIII and ice I_h have been recently calculated for the TIP4P model.[20,21] The free energy for the fluid and solid phases were calculated to determine the coexistence point by equating the chemical potential and pressure of fluid and solid phases at $T = 225$ K. Once the coexistence pressure was located at this temperature, Gibbs-Duhem simulations[22] were performed to obtain the full melting line. Further details are given elsewhere.[20,21] In Fig. 7 the melting curves of ice I_h and VIII for the TIP4P models are presented. It should be stressed that the melting curves presented in this figure at low temperatures are not extrapolations of the melting curves obtained at high temperatures, but rather calculations obtained by integrating the Clapeyron equation (Gibbs-Duhem integration). This is possible because, unlike the experimental situation where supercooled liquids freeze, nucleation for anything other than simple liquids (see Refs. 23 and 24), is rare in typical computer simulation studies.

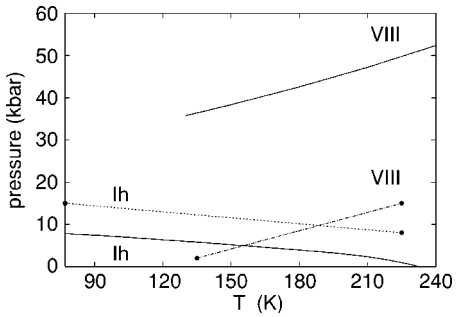

FIG. 7. Extension of the thermodynamic equilibrium melting curves (solid lines) along with the limits of stability obtained by changing the pressure along isotherms, both for ice I_h (dotted line) and ice VIII (dot-dashed line).

It is interesting to establish the range of pressures for which the solid phase exists as a metastable phase. Note that in computer simulations of bulk solids, the solid rarely melts at the equilibrium coexistence point, requiring the formation of a fluid nucleus or disordered region within the solid. The formation of such a nucleus is an activated process.[23,25] [Experimentally melting tends to initiate at the surface, defects (e.g., voids[26]) or impurities] Isothermal melting is delayed to higher (ice I_h), or lower (ice VII, ice VIII) pressures. In Fig. 7 the first pressure (the stability limit pressure) at which spontaneous melting of ice VIII occurs upon expansion is presented for $T = 135$ K and for $T = 225$ K. For orientation, a section of the phase diagram of water for the TIP4P model is presented in Fig. 8.[20,21] The equilibrium coexistence pressure for these two temperatures is ≈ 37 and 50 kbars, respectively. Therefore, ice VIII is metastable down to 35 kbar below its equilibrium coexistence pressure. In Fig. 7 we also present the first pressure at which spontaneous melting of ice I_h occurs during the compression simulations (for $T = 77$ K and for $T = 225$ K). At $T = 225$ K ice I_h is mechanically stable up to $p = 7$ kbars (at least for 3×10^5 Monte Carlo cycles). At $p = 8$ kbars ice I_h is found to melt. The coexistence pressure at this temperature is of the order of 1 kbar. [Note that the vapor-liquid-I_h triple point temperature[20,27] for the TIP4P model is $T = 232(5)$ K] At $T = 77$ K, the coexistence pressure is ≈ 8 kbars. A solid/amorphous transition occurs continuously between $p = 10$ and $p = 15$ kbars. By $p = 15$ kbars the system is completely disordered. Thus the pressure range of metastability for ice I_h is ≈ 7 kbars for the two temperatures considered.

To explore the possibility of formation of amorphous phases by decompression in other solid structures, several ices were decompressed to zero pressure along the $T = 150$ K isotherm. For ices II, III, IV, V, and VI no melting was observed. This leads to the conclusion that no amorphous phases can be expected to form upon expansion of these phases. However, a recent publication[20] hints at the possibility of forming amorphous phases upon compression of these ices.

IV. SUMMARY

In this work N-p-T computer simulations have been performed for several ice phases (namely, VII, VIII, and I_h)

using the TIP4P model of water. It has been shown that it is possible to obtain the amorphous water phases, not only from ice I_h (the usual route, both experimentally and in computer simulations) but also from other ice polymorphs. The following conclusions can be obtained from this work.

(1) At $T=135$ K and $p=1$ bar the density, energy, and structural properties, as given by the pair correlation functions of HDA obtained from ices VII and VIII, are fully consistent with those of the HDA phase obtained from the traditional route (compression of ice I_h at $T=77$ K).[3,15] When liquid water is cooled along its ice I_h melting line followed by isothermal expansion at $T=135$ K a HDA phase is also obtained. However, isobaric cooling of water at $p=1$ bar does not result in a HDA phase.

(2) A necessary (although not necessarily sufficient) condition for the formation of low temperature amorphous phases by varying the pressure is that the equilibrium melting curve of the corresponding ice is crossed.

(3) In computer simulations of bulk solid phases melting does not occur spontaneously at the equilibrium melting condition. Only rigorous free energy calculations can determine the equilibrium coexistence point.[20] It has been recently shown that ices can be overheated[28] to around 90 K beyond the equilibrium coexistence temperature (at constant pressure). Here it is shown that at constant temperature melting can be analogously delayed to higher (ice I_h) or lower (ice VIII) pressures. Note that such delayed melting is a general feature in computer simulations; also occurring for the simpler Lennard-Jones model,[23] nitromethane,[26] and various metallic elements.[24] In simulations melting occurs typically via the formation of a fluid nucleus, this being an activated process. Tse, Shpakov, and Belosludov[29] have suggested that the mechanism for amorphisation of ice VIII is the violation of the Born stability condition. The range of pressures for which the solid is metastable seems to depend weakly on temperature, and more strongly on the nature of the solid phase under consideration.

ACKNOWLEDGMENTS

This research was funded by Project Nos. FIS2004-06227-C02-02 and BFM-2001-1017-C03-02 of the Spanish DGI (Direccion General de Investigacion). One of the authors (C.M.) would like to thank the Comunidad de Madrid for the award of a postdoctoral research grant (part funded by the European Social Fund). E.S. would like to thank the Spanish Ministerio de Educacion for the award of a FPU grant.

[1] O. Mishima, L. D. Calvert, and E. Whalley, Nature (London) **310**, 393 (1984).
[2] J. S. Tse and M. L. Klein, Phys. Rev. Lett. **58**, 1672 (1987).
[3] J. S. Tse, J. Chem. Phys. **96**, 5482 (1992).
[4] O. Mishima, Nature (London) **384**, 546 (1996).
[5] D. D. Klug, Y. P. Handa, J. S. Tse, and E. Whalley, J. Chem. Phys. **90**, 2390 (1989).
[6] P. G. Debenedetti, J. Phys.: Condens. Matter **15**, R1669 (2003).
[7] S. Yashonath and C. N. R. Rao, Mol. Phys. **54**, 245 (1985).
[8] M. Parrinello and A. Rahman, Phys. Rev. Lett. **45**, 1196 (1980).
[9] W. L. Jorgensen, J. Chandrasekhar, J. D. Madura, R. W. Impey, and M. L. Klein, J. Chem. Phys. **79**, 926 (1983).
[10] D. Frenkel and B. Smit, *Understanding Molecular Simulation* (Academic, London, 1996).
[11] V. F. Petrenko and R. W. Whitworth, *Physics of Ice* (Oxford University Press, New York, 1999).
[12] W. F. Kuhs, J. L. Finney, C. Vettier, and D. V. Bliss, J. Chem. Phys. **81**, 3612 (1984).
[13] L. Pauling, J. Am. Chem. Soc. **57**, 2680 (1935).
[14] V. Buch, P. Sandler, and J. Sadlej, J. Phys. Chem. B **102**, 8641 (1998).
[15] I. Okabe, H. Tanaka, and K. Nakanishi, Phys. Rev. E **53**, 2638 (1996).
[16] R. Martoňák, D. Donadio, and M. Parrinello, Phys. Rev. Lett. **92**, 225702 (2004).
[17] B. Guillot and Y. Guissani, J. Chem. Phys. **119**, 11740 (2003).
[18] N. Giovambattista, H. E. Stanley, and F. Sciortino, cond-mat/0403365.
[19] T. Morishita, Phys. Rev. Lett. **93**, 055503 (2004).
[20] E. Sanz, C. Vega, J. L. F. Abascal, and L. G. MacDowell, Phys. Rev. Lett. **92**, 255701 (2004).
[21] E. Sanz, C. Vega, J. L. F. Abascal, and L. G. MacDowell, J. Chem. Phys. **121**, 1165 (2004).
[22] D. A. Kofke, J. Chem. Phys. **98**, 4149 (1993).
[23] S.-N. Luo, A. Strachan, and D. C. Swift, J. Chem. Phys. **120**, 11640 (2004).
[24] S.-N. Luo, T. J. Ahrens, T. Cagin, A. Strachan, W. A. Goddard III, and D. C. Swift, Phys. Rev. B **68**, 134206 (2003).
[25] G. Norman and V. Stegailov, Mol. Simul. **30**, 397 (2004).
[26] P. M. Agrawal, B. M. Rice, and D. L. Thompson, J. Chem. Phys. **119**, 9617 (2003).
[27] G. T. Gao, X. C. Zeng, and H. Tanaka, J. Chem. Phys. **112**, 8534 (2000).
[28] C. McBride, C. Vega, E. Sanz, L. G. MacDowell, and J. L. F. Abascal, Mol. Phys. (in press).
[29] J. S. Tse, V. P. Shpakov, and V. R. Belosludov, J. Chem. Phys. **111**, 11111 (1999).